Translational Oncology 25 (2022) 101500

Contents lists available at ScienceDirect

Translational Oncology

journal homepage: www.elsevier.com/locate/tranon

Original Research

MTA1-TJP1 interaction and its involvement in non-small cell lung cancer metastasis

Wei Wang [a,b,1], Mingsheng Ma [c,1], Li Li [d,1], Yunchao Huang [a], Guangqiang Zhao [a], Yongchun Zhou [e], Yantao Yang [a], Yichen Yang [a], Biying Wang [a], Lianhua Ye [a,*]

[a] Department of Thoracic Surgery, The Third Affiliated Hospital of Kunming Medical University, No. 519 Kunzhou Road, Xishan District, Kunming, Yunnan, China
[b] Department of Thoracic Surgery, Taihe Hospital (Hubei University of Medicine), Shiyan, China
[c] Department of Thoracic Surgery, The Sixth Affiliated Hospital of Kunming Medical University, Yuxi, China
[d] Biotherapy Center, The Third Affiliated Hospital of Kunming Medical University, Kunming, China
[e] Molecular Diagnosis Center, Yunnan Cancer Hospital, Kunming, China

ARTICLE INFO

Keywords:
MTA1
Non-small cell lung cancer
Metastasis
TJP1
Adhesion

ABSTRACT

Distant metastasis is the main cause of death in non-small cell lung cancer (NSCLC) patients. The mechanism of metastasis-associated protein 1(MTA1) in NSCLC has not been fully elucidated. This study aimed to reveal the mechanism of MTA1 in the invasion and metastasis of NSCLC.

Bioinformatics analysis and our previous results showed that MTA1 was highly expressed in NSCLC tissues and correlated with tumor progression. Knockout of MTA1 by CRISPR/Cas9 significantly inhibited the migration and invasion of H1299 cells, but enhanced cell adhesion. Stable overexpression of MTA1 by lentivirus transfection had opposite effects on migration, invasion and adhesion of A549 cells. The results of *in vivo* experiments in nude mouse lung metastases model confirmed the promotion of MTA1 on invasion and migration. Tight junction protein 1 (TJP1) was identified by immunoprecipitation and mass spectrometry as an interacting protein of MTA1 involved in cell adhesion. MTA1 inhibited the expression level of TJP1 protein and weakened the tight junctions between cells. More importantly, the rescue assays confirmed that the regulation of MTA1 on cell adhesion, migration and invasion was partially attenuated by TJP1.

In Conclusion, MTA1 inhibits the expression level of TJP1 protein co-localized in the cytoplasm and membrane of NSCLC cells, weakens the tight junctions between cells, and changes the adhesion, migration and invasion capabilities of cells, which may be the mechanism of MTA1 promoting the invasion and metastasis of NSCLC. Thus, targeting the MTA1-TJP1 axis may be a promising strategy for inhibiting NSCLC metastasis.

Introduction

According to the 2020 Global Cancer Epidemiological Statistics, the number of new cases of lung cancer accounted for 11.4% of the total cancer incidence, and lung cancer was the leading cause of cancer-related deaths worldwide (18.0% of the total cancer deaths) [1]. Non-small cell lung cancer (NSCLC) accounts for 80–85% of lung cancers [2]. Distant metastasis is the main cause of death in NSCLC patients, the molecules related to lung cancer metastasis have become the focus of current lung cancer research [3].

Metastasis-associated protein 1 (MTA1) was first discovered in 1994, and previous studies have found that MTA1 expression is closely related to the metastatic potential of breast cancer [4]. MTA1 expression levels are well correlated with tumor aggressiveness and its poor prognosis for patients [5,6]. In breast cancer cells, MTA1 regulates the expression of IGFBP3 in a DNMT3a-dependent and -independent manner, and the MTA1-DNMT3a-IGFBP3 axis plays an important role in breast cancer progression [7]. MTA1 can also contribute to tumor metastasis by modulating SMAD7, a key inhibitor of the TGF-β signaling pathway, resulting in altered expression of SMAD7 downstream targets [8]. MTA1 enhances epithelial-mesenchymal transition through an ErbB2-dependent pathway and promotes hepatoma cell invasion and metastasis [9]. The MTA1-S100A4-NMIIA axis promotes prostate cancer tumor cell growth and metastasis as a new way to promote tumor

* Corresponding author.
E-mail address: lhye1204@aliyun.com (L. Ye).
[1] These authors contributed equally to this work.

https://doi.org/10.1016/j.tranon.2022.101500
Received 24 April 2022; Received in revised form 18 July 2022; Accepted 27 July 2022
Available online 6 August 2022

angiogenesis [10]. MTA1 is an important molecule in the process of invasion and metastasis of various cancers, and its mechanism of action is different in different cancers.

Our recent study found that MTA1 protein expression can stratify the risk of disease progression in patients with multifocal NSCLC ≤3 cm, and found that MTA1 protein was positively expressed in the cytoplasm of NSCLC tissues [11]. Previous studies mostly believed that MTA1 plays a role in promoting cancer through transcriptional co-regulators [5,6], while the role of cytoplasmic MTA1 in NSCLC has not yet been elucidated. In this study, we attempted to clarify the role of MTA1 in the invasion and metastasis of NSCLC using CRISPR/Cas9 and lentivirus transfection techniques, identify and screen MTA1 interacting proteins that play an important role in NSCLC invasion and metastasis, and reveal the mechanism of MTA1 and its interacting proteins in NSCLC invasion and metastasis.

Materials and methods

Cell lines and mice

The NSCLC cell lines NCI-H1299, NCI-H292 and NCI-H838 used in this study were purchased from the Cell bank of Chinese Academy of Sciences. A549, SK-MES-1, NCI-H1734, XWLC-05 and 293T cells were donated by Yunnan Provincial Key Laboratory of Lung Cancer Research. Six-week-old male BALB/c-nu mice were purchased from Animal Center of Kunming Medical University. The mice were used according to the protocol approved by Animal Experiment Ethics Review Committee of Kunming Medical University.

MTA1 knockout

LentiCRISPR v2 vector and packaging plasmids psPAX2, pMD2.G were purchased from Xinghua Yueyang Biotechnology Company (Beijing, China). The MTA1-CRISPR/Cas9 KO plasmid consists of a LentiCRISPR V2 vector and a target-specific guide RNA (gRNA) designed for knockout of MTA1. The sequences of three gRNAs were as follows:

gRNA#1 5′-GATAAAGGAGAGATTCGAGTAGG-3′,
gRNA#2 5′-TGGCCGAGACCAGTCCAGGTTGG-3′,
gRNA#3 5′-GCAGTCCAGGGCCCGTGCGAAGG-3′.

MTA1-CRISPR/Cas9 KO plasmid or Control CRISPR/Cas9 plasmid and packaging plasmids psPAX2, pMD2.G were co-transfected into 293T cells using PEI transfection reagent (polysciences, USA). After 48 and 72 h, the virus fluid was collected and filtered with 0.22 μm disposable needle filter. H1299 cells were implanted into 6-well plates, and transfection began after cell convergence reached 70−80%. 1 mL of virus fluid, 1 mL of RPMI 1640 medium and 2 μL of polybrene were added to each well. 48 h after transfection, the culture medium was replaced and puromycin (2 μg/ml) was added to screen the transfected cells. Western Blot was performed to verify the knockout effect. Monoclonal cells were selected from cells with significantly reduced MTA1 expression levels, and the cells with successful MTA1 knockout were verified by Western Blot.

MTA1 overexpression

Vector plasmid pEZ-Lv201 and packaging plasmids pH1, pH2 used to construct MTA1 overexpression plasmids were purchased from Funeng genes company (Guangzhou, China). MTA1 overexpression vector EX-Z8699-Lv201 or Control vector pEZ-Lv201 and packaging plasmid pH1, pH2 were used to co-transfect 293T cells with EndoFectin™ MAX transfection reagent. After collecting the virus fluid, A549 cells were transfected, and the method was similar to that of MTA1 knockout. The successful plasmid transfection was verified under a fluorescence microscope. Cells with successful MTA1 overexpression were verified by Western Blot and qPCR.

Protein extraction and Western Blot analysis

Cells were lysed in RIPA buffer. Proteins were separated via 8% sodium dodecyl sulfate-polyacrylamide gel electrophoresis (SDS-PAGE), transferred to poly vinylidene fluoride membranes, blocked with Tris buffered saline (TBS) containing 3% (wt/vol) nonfat milk for 1.5 h, and then incubated overnight at 4 °C with primary antibodies. After washed three times (10 min per time), membrane was incubated with horseradish peroxidase (HRP)-conjugated IgG secondary antibodies (1:3000) at room temperature for 1 h. After immersion with immobilon Western HRP chemiluminescence reagent, the bands were visualized and quantified by ImageJ software (National Institutes of Health, USA). The antibodies used in the study were: MTA1 (CST, #5647, 1:1000), tight junction protein 1(TJP1) (CST, #6487,1:1000), β-Actin (ABclonal, AC026,1:50,000).

RNA extraction and qPCR

Total RNA was isolated from cells using RNA-easy™ Isolation Reagent (Vazyme, China) according to the manufacturer's recommendation. Then 1 μg of mRNA were used to synthesize cDNA by using HiScript III RT SuperMix (Vazyme). The qPCR was performed on Real-time Fluorescence Quantitative PCR System (Thermo, USA) with ChamQ Universal SYBR qPCR Master Mix (Vazyme). Primers used in the study were:

MTA1 Forward 5′ -ACGCAACCCTGTCAGTCTG-3′,
MTA1 Reverse 5′-GGGCAGGTCCACCATTTCC-3′.
TJP1 Forward 5′-TAACAGAAGGAGTGAGAAGATTTG-3′,
TJP1 Reverse 5′-TGTGACTTTAGTAGGTTTAGCAGG-3′.
GAPDH Forward 5′-GGAGCGAGATCCCTCCAAAAT-3′,
GAPDH Reverse 5′-GGCTGTTGTCATACTTCTCATGG-3′.

The cycle number at threshold was used to quantify the levels of genes. Transcripts of GAPDH in the same incubations were used for normalization. The relative expression levels of genes were calculated by the 2-ΔCt methods.

Transwell migration assay

4×10^4 cells per well were seeded in the upper chamber of the Transwell chamber, and 600 μL of 20% fetal bovine serum (FBS)-supplemented RPMI 1640 medium in the lower chamber. After 24 h of culture, the cells in the upper chamber were wiped off, fixed with 4% paraformaldehyde for 20 min, stained with 0.5% crystal violet solution for 1 h. Photographs were taken under an inverted microscope, and the average of the number of cells in 5 fields of view was counted.

Transwell invasion assay

Transwell chambers were coated with diluted Matrigel gel (250 μg/mL), and 8×10^4 cells per well were seeded in the upper chamber. After 48 h of culture, taken pictures and counted the number of penetrating cells. The rest of the steps are the same as in the Transwell migration assay.

Wound-healing assay

Cells were seeded into 6-well plates and scratched when they had grown to about 90% confluence. After washing with phosphate buffered saline (PBS), the cells were incubated in 1% FBS-supplemented RPMI 1640 medium. Photographs were taken at 0 h, 12 h and 24 h after scratching, respectively. Scratch width (W) was calculated with Image J software, W = area of scratch/length of scratch, wound healing rate =

(initial W - W after culture)/initial $W \times 100\%$.

Adhesion assay

Artificial basement membrane was prepared by coating a 96-well plate with diluted Matrigel (BD, USA) (40 μg/ml) and air-dried overnight. 2×10^3cells per well were seeded in, and cultured for 1 h at 37 °C with a constant-temperature shaker at a speed of 80 rpm/min. Non-adherent cells were washed away with PBS and photographed under a microscope. 100 μl of 10% FBS-supplemented RPMI 1640 medium and 10 μl of CCK-8 working solution was added to each well, and the optical density value at 450 nm was measured after incubating for 2 h.

In vivo tumor metastasis

5×10^6 MTA1 knockout or negative control H1299 cells were injected into the right atrium of nude mice (9 per group). After 6 weeks, the lung tissues were dissected out, the lung nodules were counted and the metastasis index was calculated using methods reported in previous study [12]. The lung tissue was fixed with 4% paraformaldehyde and stained with hematoxylin-eosin. The metastatic tumor tissue was embedded in paraffin for immunohistochemistry (IHC).

Human and nude mice tissue IHC

Fresh human non-small cell lung cancer tissues and normal lung tissues were obtained from the specimen bank of the Yunnan Provincial Key Laboratory of Lung Cancer Research. This study was approved by the Ethics Committee of the Third Affiliated Hospital of Kunming Medical University (NO. KY2020160), and informed consent was waived. The expression levels of MTA1 and TJP1 in human and nude mouse tumor tissues were evaluated by IHC methods. IHC staining and semi-quantitative immunoreactivity scoring methods for MTA1 expression were similar to our previous study [11]. The expression level of TJP1 was evaluated by the average gray value using Image-Pro-Plus 6.0 software [13].

Immunoprecipitation (IP)

H1299 cells were lysed with IP lysis buffer containing protease inhibitors, and the protein supernatant was divided into 3 parts: experimental group, IgG group and input (300 μL per group). 8 μL of MTA1 and IgG were conjugated with 100 μL of DynabeadS™ protein G (Thermo, USA) on a magnetic frame, respectively. Then, the proteins of experimental group and IgG group were added to the MTA1 and IgG antibody conjugates, respectively. The target proteins were captured on the magnetic frame. Magnetic beads-antibody-target protein complexes and input were denatured and then subjected to SDS-PAGE, stained with Coomassie brilliant blue staining solution for 5 h, shaken on a shaker to decolorize, and photographed with a scanner.

Mass spectrometry (MS)

SDS-PAGE was performed before MS and stained with a silver staining kit (Qiyuan Biotechnology, China). The gel bands were minced, destained, dehydrated, and digested, and the peptides were analyzed by LC-MS using Thermo Scientific™Q Exactive Plus mass spectrometer (Thermo, USA). Protein identification was performed using Proteome Discoverer 1.3 database [14].

Immunofluorescent staining

5×10^4 cells were seeded on cell slides in 24-well plates. When the cells grew to 60–70% confluent, they were fixed with 4% paraformaldehyde for 20 min and incubated with 0.3% Triton X-100 solution for 20 min. Add 200 μL of rabbit anti-MTA1 and mouse anti-TJP1 (diluted 1:100 with 2% BSA) and incubate overnight at 4 °C. Add 200 μL of Alexa Fluor™ 488 Goat Anti-rabbit IgG (green) and Goat Anti-mouse IgG (red) monoclonal secondary antibody (1:500, Invitrogen, USA), incubated at 37 °C for 40 min. Nuclear counterstaining was performed with 200 μL of DIPA (1:1000 dilution with 1 × PBS). Images were acquired with a laser confocal microscope (ZEISS, Germany) after mounting with anti-fluorescence quenching.

Bioinformatics methods

NSCLC transcriptome data from The Cancer Genome Atlas (TCGA) database were obtained to analyze the difference of MTA1 expression level between cancer tissues and lung tissues. The significance of MAT1 expression on the prognosis of NSCLC patients was obtained from the Kaplan Meier Plotter database. Gene Ontology (GO) enrichment analysis was performed on the MTA1 interacting proteins identified by MS using DAVID tool. The intersection of molecules significantly enriched in the three functional categories of molecular biological function (MF), biological process (BP) and cytological components (CC) with NSCLC differentially expressed genes in the TCGA database, and the correlation between candidate molecules and MTA1 mRNA expression was analyzed by using NSCLC transcriptome data in the TCGA database.

Further combined with the scoring of MS-identified proteins, the MTA1-interacting proteins that may be involved in the invasion and metastasis of NSCLC were preliminarily screened.

Statistical analysis

Statistical Package of Social Sciences version 23.0 (IBM Corp, USA) and GraphPad Prism8 (GraphPad Software, USA) were used to perform statistics and analysis of the data. The normally distributed measurement data was described as $\bar{x} \pm s$ from at least three independent experiments. For statistical analysis, two-tailed unpaired *t*-test between two groups and ANOVA followed by SNK test for multiple comparison were performed. The non-normally distributed measurement data was described as *M* and *R*, and Mann-Whitney test was used to analyze differences between groups. $P < 0.05$ was considered to be statistically significant.

MTA1 plays an important role in the progression of NSCLC

Previous studies have shown that MTA1 is an important molecule in the invasion and metastasis of various cancers. We first used the database to analyze the expression and significance of MTA1 in NSCLC. Transcriptome analysis of TCGA showed that the level of MTA1 mRNA expression in lung squamous cell carcinoma and lung adenocarcinoma tissues was significantly higher than that in normal lung tissues (Fig. 1A, B). Kaplan Meier Plotter data showed that the progression-free survival (PFS) and overall survival (OS) of NSCLC patients with high MAT1 expression were inferior to those of patients with low MAT1 expression (Fig. 1C, D). Next, IHC was performed, and the results showed that MTA1 protein was negative expression in normal lung tissues (Fig. 1E), positive in NSCLC cancer tissues (Fig. 1F), and strongly positive in metastatic lymph nodes (Fig. 1G). MTA1 protein was positively expressed in both nucleus and cytoplasm of cancer tissues (Fig. 1H). These results suggest that MTA1 plays an important role in the progression of NSCLC.

MTA1 promotes the invasion and metastasis of NSCLC

To clarify the role of MTA1 in NSCLC progression, we first examined the level of MTA1 protein expression in 7 NSCLC cells. Western Blot results showed that the level of MTA1 protein expression was the highest in H1299 cells and the lowest in H1734 cells (Supplementary Fig. 1A, B). CRISPR/Cas9 technique was used to knock out MTA1 in H1299 cells with the highest MTA1 expression (Supplementary Fig. 1C, D).

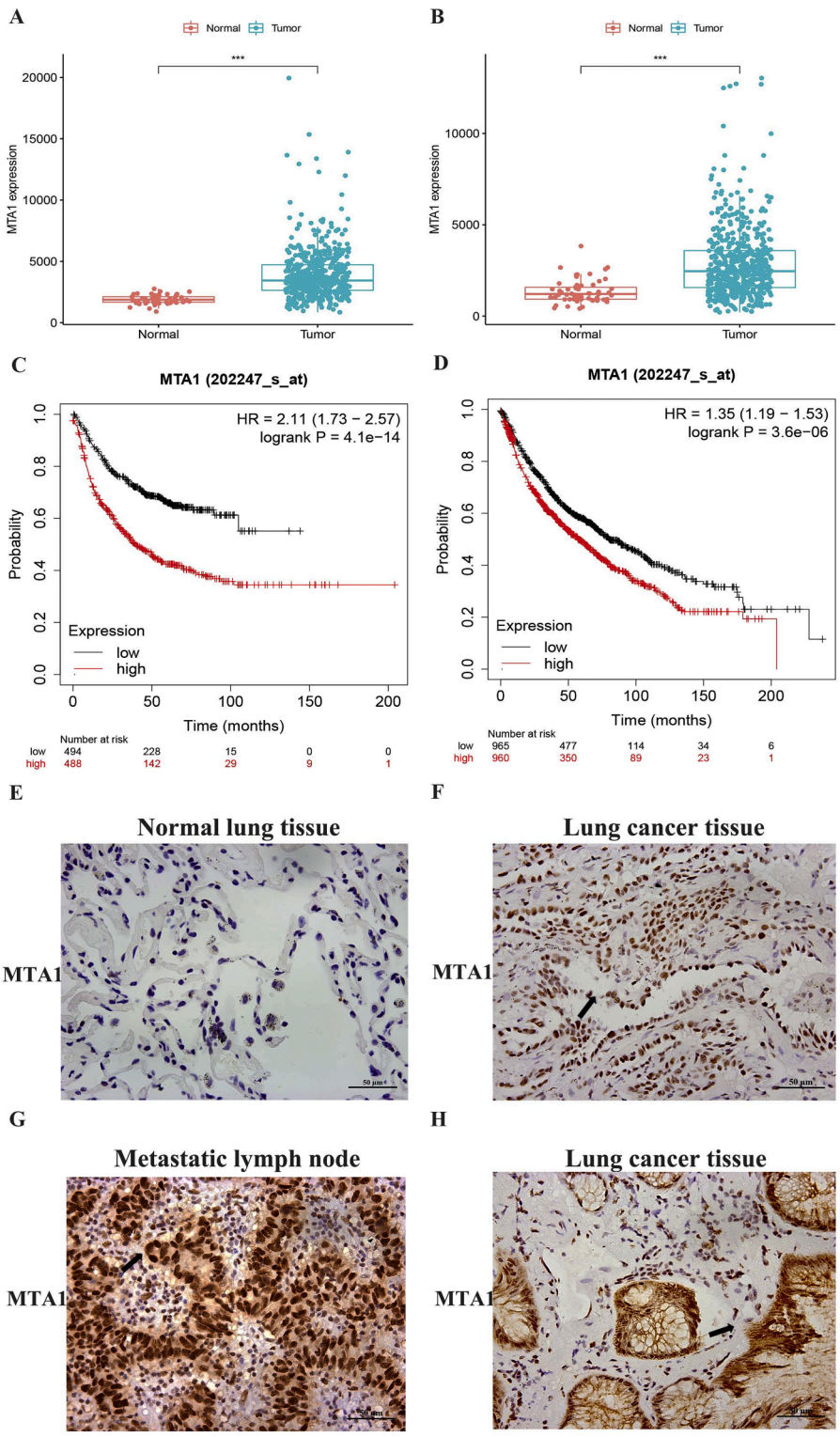

Fig. 1. MTA1 is highly expressed in non-small cell lung cancer (NSCLC) tissues and is associated with poor prognosis of patients. (A) The level of MTA1 mRNA expression in squamous cell carcinoma is higher than that in normal lung tissue of lung cancer patients in The Cancer Genome Atlas (TCGA) database. ***$P < 0.001$, *t*-test. (B) The level of MTA1 mRNA expression in adenocarcinoma tissues is higher than that in normal lung tissues of lung cancer patients in TCGA database. ***$P < 0.001$, *t*-test. (C) MAT1 mRNA expression level predicts poor progression-free survival of NSCLC patients in the Kaplan Meier Plotter database. (D) MAT1 mRNA expression level correlates with worsening overall survival of NSCLC patients in the Kaplan Meier Plotter database. (E) Representative images of negative MTA1 protein expression in lung tissue. (F) Representative images of positive MTA1 protein expression in lung cancer tissue. (G) Representative images of strongly positive MTA1 protein expression in metastatic lymph nodes. (H) Representative image of positive MTA1 protein expression in both nucleus and cytoplasm of lung cancer tissue.

Lentivirus transfection technique was used to overexpress MTA1 in A549 cells with low MTA1 expression (Supplementary Fig. 1E–G), and cell function assay was conducted after cell model was successfully constructed. Wound-healing assay was used to evaluate the lateral migration ability of the cells. It was found that knockout of MTA1 significantly inhibited the lateral migration of H1299 cells (Fig. 2A, C), and overexpression of MTA1 significantly promoted the lateral migration of A549 cells (Fig. 2B, D). The results of Transwell migration assay showed that knockout of MTA1 significantly inhibited the longitudinal migration of H1299 cells (Fig. 2E), while overexpression of MTA1 significantly promoted the longitudinal migration of A549 cells (Fig. 2F). The results of Transwell invasion assay showed that knockout of MTA1 significantly inhibited the invasion of H1299 cells (Fig. 2G), while overexpression of MTA1 significantly promoted the invasion of A549 cells (Fig. 2H). Artificial basement membranes were prepared by coating 96-well plates with Matrigel to assess cell adhesion. MTA1 knockout H1299 cells showed higher levels of adhesion than control cells (Fig. 2I), whereas MTA1 overexpression inhibited the adhesion of

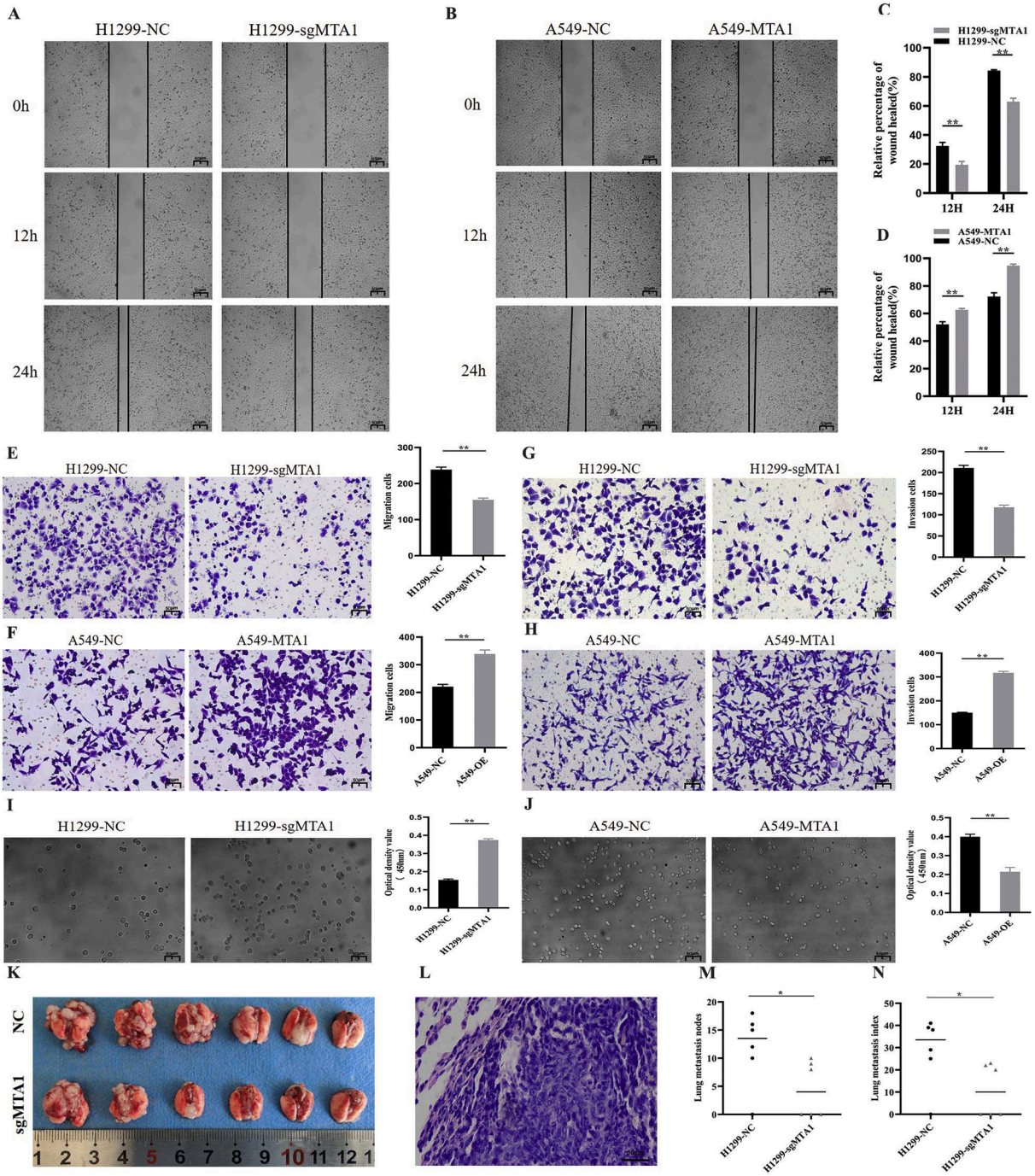

Fig. 2. MTA1 promotes the invasion and metastasis of non-small cell lung cancer. (A) Knockout of MTA1 inhibits lateral migration of H1299 cells as measured by wound-healing assays. The wound edges are indicated by black lines. Representative images are shown. (B) Overexpression of MTA1 promotes lateral migration of A549 cells as measured by wound-healing assays. The wound edges are indicated by black lines. Representative images are shown. (C), (D) The quantitative results of (A) and (B), respectively. The y axis represents percentage of wound healed. Every experimental group is compared with the NC group. Error bars represent *SD* from 3 repeats. $^{**}P < 0.01$, *t*-test. (E) Knockout of MTA1 inhibits longitudinal migration of H1299 cells as measured by Transwell migration assays. (F) Overexpression of MTA1 promotes longitudinal migration of A549 cells as measured by Transwell migration assays. (G) Knockout of MTA1 inhibits invasion of H1299 cells as measured by Transwell invasion assays. (H) Overexpression of MTA1 promotes invasion of H1299 cells as measured by Transwell invasion assays. (E)-(H) Representative images are shown. The quantitative results from 3 replicate experiments. The y axis represents number of transwell cells. Every experimental group is compared with the NC group. Error bars represent *SD*. $^{**}P < 0.01$, *t*-test. (I) Knockout of MTA1 promotes adhesion of H1299 cells as measured by cell adhesion assays. (J) Overexpression of MTA1 inhibits adhesion of A549 cells as measured by cell adhesion assays. (I)-(J) Representative images are shown. The quantitative results from 3 replicate experiments. The y axis represents optical density values of adherent cells. Every experimental group is compared with the NC group. Error bars represent *SD*. $^{**}P < 0.01$, *t*-test. (K) Knockout of MTA1 inhibits H1299 cells from forming lung metastases in nude mice. (L) The formation of lung metastases is confirmed by pathological hematoxylin-eosin staining. (M) The number of lung metastasis nodes of nude mice in the MTA1 knockout group is less than that in the NC group. Data analyzed is the median of the number of lung metastasis nodes ($n = 6$), Mann-Whitney test, $^{*}P < 0.05$. (N) The lung metastasis index of nude mice in the MTA1 knockout group is less than that in the NC group. Data analyzed is the median of lung metastasis index ($n = 6$), Mann-Whitney test, $^{*}P < 0.05$.

A549 cells (Fig. 2J).

Next, we validated the function of MTA1 in invasion and metastasis *in vivo*. MTA1 knockout H1299 cells and control cells were injected into the right atrium of nude mice to establish lung metastases models. After 6 weeks, the nude mice were dissected and the lung tissues were completely removed to evaluate the effect of MTA1 on metastasis. Three nude mice in the MTA1 knockout group (H1299-sgMTA1) developed lung metastases, and five nude mice in the control group (H1299-NC) developed lung metastases (Fig. 2K). The lung nodules of nude mice were confirmed to be lung metastases by pathological HE staining (Fig. 2L). The number of lung metastasis nodes and the lung metastasis index of nude mice in the H1299-sgMTA1 group were lower than those in the H1299-NC group (Fig. 2M, N). Taken together, these results suggest that MTA1 promotes the invasion and metastasis of NSCLC.

TJP1 is an interacting protein of MTA1 involved in cell adhesion

In order to identify the interacting proteins of MTA1, the H1299 cells with high abundance of endogenous MTA1 protein were used to extract proteins for IP. The magnetic bead-antibody-target protein complexes captured by MTA1 antibody and IgG antibody were sent to MS for detection, and the quality of the samples was evaluated before the detection. The silver staining results after SDS-PAGE showed that the bands of MTA1 antibody and IgG antibody were significantly different (Fig. 3A). 951 MTA1-interacting proteins were identified by MS from IP products (Supplementary Table 1). GO enrichment analysis of the identified MTA1-interacting proteins revealed that the cell adhesion related proteins were significantly enriched in BP, MF and CC (Fig. 3B-D). 46 proteins involved in cell adhesion were obtained by intersecting the proteins enriched in BP, MF and CC (Fig. 3E). Next, differential expression analysis and correlation analysis were performed using TCGA transcriptome data, and MTA1-interacting proteins were screened in combination with the scores of MS-identified proteins. 46 proteins involved in cell adhesion were intersected with differentially expressed genes of NSCLC in the TCGA database to obtain 11 candidate molecules (Fig. 3F). Using NSCLC transcriptome data in TCGA to analyze the correlation between these 11 candidate molecules and MTA1 mRNA expression levels, it was found that LDHA, CKAP5, TJP1, and MTA1 mRNA expression levels were positively correlated. (TJP1: $r = 0.33$, $P < 0.01$; LDHA: $r = 0.34$, $P < 0.01$; CKAP5: $r = 0.56$, $P < 0.01$) (Fig. 3G-I). According to the identification results of mass spectrometry (Supplementary Table 1), TJP1 with the highest protein score (TJP1: 309.75, LDHA: 207.77, CKAP5: 141.76) in LDHA, CKAP5 and TJP1. Next, the immunoprecipitated products were detected by Western Blot, and the results showed TJP1 was an interacting protein of MTA1 (Fig. 3J). Western Blot results showed that the level of TJP1 protein expression was the highest in H1734 cells and the lowest in H838 cells (Supplementary Fig. 1H, I). IHC results showed that TJP1 protein was strongly positive expressed in normal lung tissue and weakly positive expressed in NSCLC tissue (Fig. 3K). Our previous results indicated that MTA1 protein expression was higher in NSCLC cancer tissues than in normal lung tissues [11]. The above results indicate that TJP1 is an interacting protein of MTA1, and there may be a negative regulatory relationship between TJP1 protein and MTA1 protein.

MTA1 regulates the expression of TJP1 protein and alters tight junctions between cells

The subcellular localization of MTA1 protein and TJP1 protein in H1299 and H292 cells with high expression of endogenous MTA1 protein was determined by immunofluorescence assay. The co-localization of MTA1 protein and TJP1 protein in the cytoplasm and cell membrane of H1299 cells and H292 cells could be clearly observed by laser confocal microscopy (Fig. 4A). Inverse IP results further confirmed the direct interaction of MTA1 protein with TJP1 protein (Fig. 4B). To further clarify the regulatory relationship between MTA1 and TJP1, we successfully constructed H1299 cells with knockdown of TJP1 using siRNA (Supplementary Fig. 1 J, K). Western Blot results showed that the level of TJP1 protein expression was significantly decreased after overexpression of MTA1, and the level of TJP1 protein expression was significantly increased after knockout of MTA1, however, there was no significant change in MTA1 protein expression level after knockdown of TJP1 (Fig. 4C-F). Interestingly, no significant regulatory relationship was found between MTA1 and TJP1 at mRNA level (Fig. 4G, H), suggesting that the regulatory effect of MTA1 on TJP1 expression may not be achieved through transcriptional regulation. The IHC results of nude mouse lung metastases showed that the level of MTA1 protein expression in the MTA1 knockout group (H1299-sgMTA1) was lower than that in the control group (H1299-NC) (Fig. 4I, K). However, the level of TJP1 protein expression in the lung metastases of nude mice in the H1299-sgMTA1 group was higher than that in the H1299-NC group (Fig. 4J, L). TJP1, Claudin1, Occludin are the main components of tight junctions [15,16], and we performed immunofluorescence to observe the effect of MTA1 on tight junctions. The results of immunofluorescence showed that the expression of TJP1, Claudin1, and Occludin at the cell junctions in the cells with MTA1 knockout (H1299-sgMTA1) were higher than that in the control cells (H1299-NC) (Fig. 5A), suggesting that MTA1 might attenuate the state of tight junctions between cells. Taken together, these results suggest that MTA1 regulates the expression of TJP1 protein and alters tight junctions between cells.

TJP1 is involved in MTA1 regulated invasion and metastasis of NSCLC cells.

In order to determine whether MTA1 promotes invasion and metastasis by regulating the expression of TJP1 protein, we used siRNA to knockdown TJP1 expression in H1299 cells with MTA1-knockout and conducted rescue assays. The promoting effect of MTA1 knockout on H1299 cell adhesion could be attenuated by TJP1 knockdown, knockdown of TJP1 inhibited the adhesion of H1299 cells (Fig. 5B, C). Meanwhile, the inhibiting effect of MTA1 knockout on the migration and invasion of H1299 cells could be attenuated by TJP1 knockdown, knockdown of TJP1 promoted the migration and invasion of H1299 cells (Fig. 5D-G). It suggested that TJP1 was involved in MTA1 regulated adhesion migration and invasion of NSCLC cells.

Discussion

MTA1 protein was first isolated and identified from MTLn3, a highly metastatic rat breast cancer cell [4]. The molecular weight of MTA1 protein is about 80 kDa, and the gene encoding MTA1 is located on chromosome 14q32 [17]. The common domains of MTA family proteins endow them with protein-protein, protein-DNA binding potential, and function in transcriptional regulation and signal transmission [18]. TCGA data showed that the mRNA expression level of MTA1 in NSCLC cancer tissues was significantly higher than that in adjacent tissues. Kaplan Meier Plotter survival analysis data showed that the OS and PFS of NSCLC patients with high MAT1 expression were worse than those of patients with low MAT1 expression. Our previous results indicated that MTA1 protein expression was higher in NSCLC cancer tissues than in normal lung tissues [11]. These results suggest that MAT1 may play an important role in the invasion and metastasis of NSCLC.

CRISPR/Cas9 technology has been widely used in the functional study of tumor-related genes [19]. We successfully knocked out MTA1 in H1299 cells using CRISPR/Cas9. Knockout of MTA1 significantly inhibited the migration and invasion of H1299 cells and enhanced cell adhesion. However, overexpression of MTA1 had the opposite effect on the migration, invasion and adhesion of A549 cells. The *in vivo* experimental results showed that MTA1 could promote the formation of lung metastases. Another study constructed a mouse model of breast cancer lung metastasis with selective MTA1 genetic deletion, and the results showed that MTA1 regulates breast cancer lung metastasis without affecting the formation of primary tumors [20], which was consistent with our results. The results of cell and *in vivo* experiments indicated that

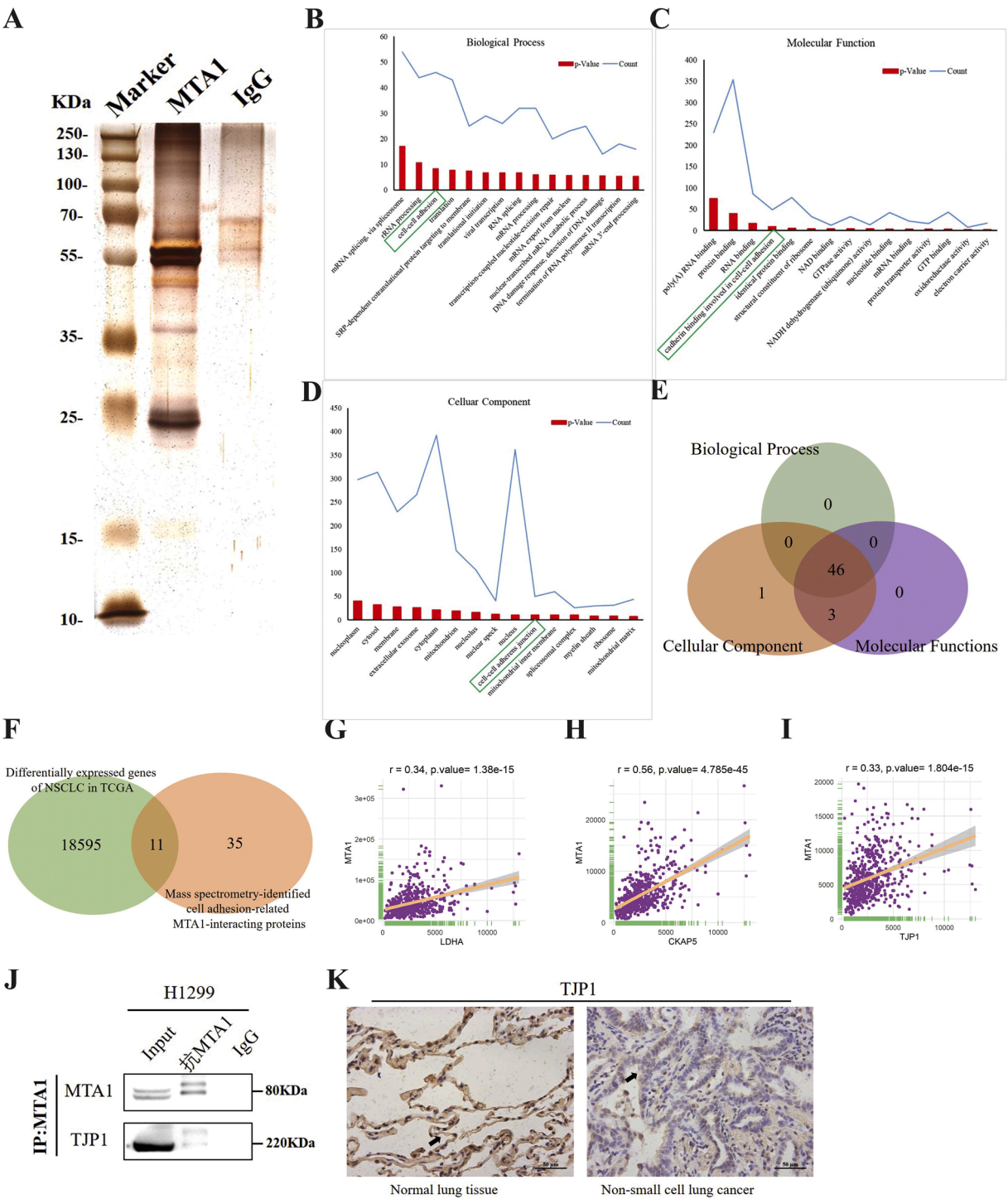

Fig. 3. TJP1 is an interacting protein of MTA1 involved in cell adhesion. (A) Silver staining shows that the protein bands captured by MTA1 antibody and IgG antibody are significantly different. (B-D) Gene Ontology enrichment analysis of MTA1 interaction proteins identified by mass spectrometry shows that cell adhesion related proteins are significantly enriched in biological process, molecular function and cellular component, respectively. (E) The enriched proteins in biological process, molecular function and cellular component are intersected to obtain 46 MTA1-interacting proteins involved in cell adhesion. (F) 46 proteins involved in cell adhesion are intersected with differentially expressed genes of NSCLC in the TCGA database to obtain 11 candidate proteins. (G-I) Correlation of TJP1, LDHA, CKAP5 and MTA1 mRNA expression in TCGA database. LDHA is correlated with MTA1 ($r = 0.34$, $P < 0.01$). CKAP5 is correlated with MTA1 ($r = 0.56$, $P < 0.01$). TJP1 is correlated with MTA1($r = 0.33$, $P < 0.01$). (J) Western Blot results shows that TJP1 is an interacting protein of MTA1. (K) TJP1, a cell adhesion-related MTA1-interacting protein, is strongly positive expressed in normal lung tissue, is weakly positive expression of TJP1 protein in non-small cell lung cancer, representative images are shown.

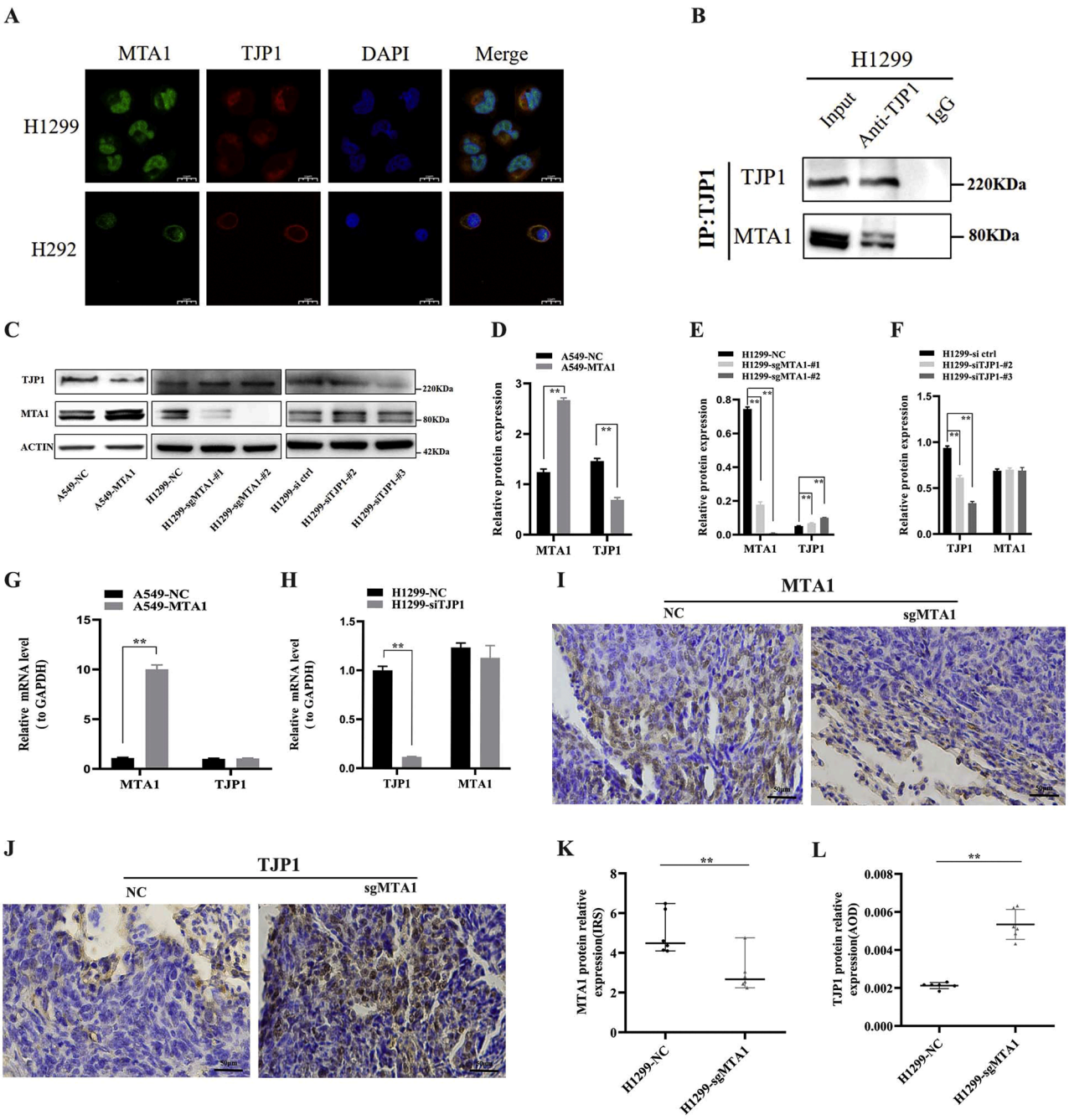

Fig. 4. MTA1 regulates the expression of TJP1 protein. (A) Immunofluorescence results confirm that MTA1 protein co-locates with TJP1 protein in the cytoplasm and cell membrane of H1299 cells and H292 cells. The yellow area indicated by the yellow arrow is the co-localization of MTA1 protein and TJP1 protein observed under the laser confocal microscope. (B) Direct interaction between MTA1 protein and TJP1 protein is demonstrated by reverse immunoprecipitation. (C) TJP1 protein expression level is significantly down-regulated with MTA1 overexpression and up-regulated with MTA1 knockout; however, there is no significant change in MTA1 protein expression level with TJP1 knockdown. Representative images of Western Blot are shown. (D-F) Quantitative analysis of (C). Error bars represent *SD* from 3 repeats, *t*-test, $^{**}P < 0.01$. (G) Overexpression of MAT1 shows no significant changes of TJP1 mRNA expression in A549 cells. (H) Knockdown of TJP1 shows no significant changes of MTA1 mRNA expression in H1299 cells. (G-H) Error bars represent SD, data from 3 independent replicates with 3 replicate wells, *t*-test, $^{**}P < 0.01$. (I) Representative images of immunohistochemical staining of MTA1 protein in the lung metastases of nude mice in MTA1 knockout group and control group. (J) Representative images of immunohistochemical staining of TJP1 protein in the lung metastases of nude mice in MTA1 knockout group and control group. (K) The level of MTA1 protein expression in lung metastases tissue of nude mice of the MTA1 knockout group (H1299-sgMTA1) was lower than that of the control group (H1299-NC). Data analyzed is the median of immunoreactivity scoring ($n = 6$), Mann-Whitney test, $^{**}P < 0.01$. (L) The level of TJP1 protein expression in lung metastases tissue of nude mice of the MTA1 knockout group (H1299-sgMTA1) was higher than that of the control group (H1299-NC). Data analyzed is the median of average optical densities value ($n = 6$), Mann-Whitney test, $^{**}P < 0.01$.

MTA1 plays an important role in the invasion and metastasis of NSCLC, which may be achieved by regulating cell adhesion, migration and invasion.

Early studies suggested that MTA1 is an important component of the nucleosome remodeling and deacetylation complex and plays an important role in transcriptional repression through histone deacetylation and chromatin remodeling [21]. Subsequent studies reported the transcriptional co-activation function of MTA1 [22–24]. Initial studies

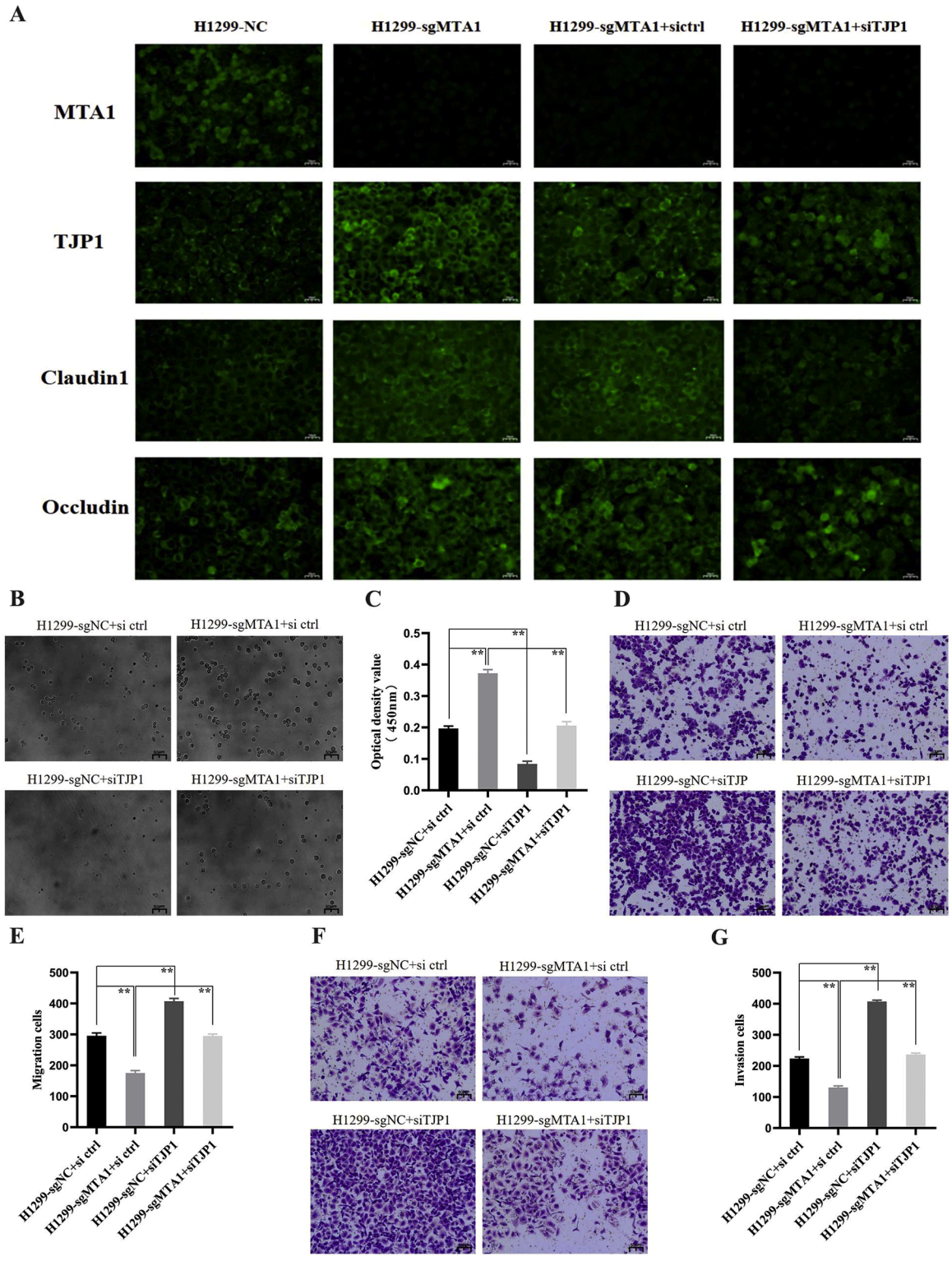

Fig. 5. Alterations of cell adhesion, migration, and invasion caused by MTA1 knockout are attenuated by TJP1 knockdown. (A) The expression of TJP1, Claudin1, and Occludin at the cell junctions in the cells with MTA1 knockout (H1299-sgMTA1) were higher than that in the control cells (H1299-NC) as measured by Immunofluorescence. (B) Knockout of MTA1 promotes adhesion of H1299 cells as measured by cell adhesion assays. Alterations caused by MTA1 knockout are attenuated by TJP1 knockdown. Knockdown of TJP1 inhibits adhesion of H1299 cells. Representative images are shown. (C) The quantitative analysis of (B). The y axis represents optical density values of adherent H1299 cells. Error bars represent *SD* from 3 repeats, *t*-test, ** $P < 0.01$. (D) Knockout of MTA1 inhibits migration of H1299 cells as measured by Transwell assays. Alterations caused by MTA1 knockout are attenuated by TJP1 knockdown. Knockdown of TJP1 promotes migration of H1299 cells. Representative images are shown. (E) The quantitative analysis of (D). The y axis represents number of Transwell cells. Error bars represent *SD* from 3 repeats, *t*-test, ** $P < 0.01$. (F) Knockout of MTA1 inhibits invasion of H1299 cells as measured by Matrigel Transwell assays. Alterations caused by MTA1 knockout are attenuated by TJP1 knockdown. Knockdown of TJP1 promotes invasion of H1299 cells. Representative images are shown. (G) The quantitative analysis of (F). The y axis represents number of Transwell cells. Error bars represent *SD* from 3 repeats, *t*-test, ** $P < 0.01$.

believed that MTA1 was only localized in the nucleus [25,26], but in recent years, studies have found that cytoplasmic MTA1 is associated with the progression of colon cancer [27]. Our results showed that MTA1 was significantly expressed in the cytoplasm of NSCLC. We used IP, MS and bioinformatics to screen out the MTA1-interacting protein—TJP1, that may be involved in cell adhesion. This suggests that the mechanism of MTA1 in the invasion and metastasis of NSCLC may be different from other tumors.

Studies at the cellular and tissue levels found that MTA1 inhibited the expression level of TJP1 protein, and MTA1 regulated the subcellular distribution of TJP1 protein and altered the tight junctions between cells. However, there was no clear regulatory relationship between MTA1 and TJP1 at mRNA level, suggesting that the mechanism of MTA1 inhibiting TJP1 expression might be regulating protein translation or post-translational modification of TJP1. The results of immunofluorescence experiments showed that MTA1 protein and TJP1 protein co-localized in the cytoplasm and membrane of NSCLC cells. The results of reverse IP also confirmed the direct interaction of MTA1 protein with TJP1 protein. One end of TJP1 is linked to the intracellular region of transmembrane proteins and the other to the cytoskeleton, and the role of TJP1 in cell proliferation, transformation and metastasis has been gradually discovered [28]. It has been shown that TJP1 isoforms can enhance the assembly of actin stress fibers and promote the migration of A549 cells [29]. TJP1, Claudin1, Occludin were the main components of tight junctions [15,16], immunofluorescence assay results in this study showed that knockout of MTA1 in H1299 cells increased the expression of TJP1, Claudin1 and Occludin at the cell junction. These results suggest that MTA1 may regulate the state of tight junctions between cells.

We knocked down TJP1 on the basis of MTA1 knockout, and performed the rescue assays of cell adhesion, migration and invasion. The results showed that the inhibitory effect of MTA1 on H1299 cell adhesion could be partially attenuated by TJP1, and the promoting effect of MTA1 on H1299 cell migration and invasion could be partially attenuated by TJP1. Kondratyeva et al. found that ectopic expression of PDX1 in pancreatic cancer cells inhibited the migratory potential of cells by increasing the adhesion of pancreatic cancer cells [30]. Cell population invasion also requires dynamic cell-to-cell adhesion, and the relaxation of cell junctions leads to invasion [31]. Taken together, MTA1 may reduce the adhesion of NSCLC cells to the extracellular matrix by inhibiting the expression level of TJP1 protein and regulating the state of tight junctions between cells, which is conducive to cell migration and invasion, and then leads to the invasion and metastasis of NSCLC.

Conclusion

In conclusion, MTA1 inhibits NSCLC cell adhesion, promotes cell migration and invasion, and promotes NSCLC cells to form lung metastases in nude mice. MTA1 inhibits the expression level of TJP1 protein co-localized in the cytoplasm and membrane of NSCLC cells, weakens the tight junctions between cells, and changes the adhesion, migration and invasion capabilities of cells, which may be the mechanism of MTA1 promoting the invasion and metastasis of NSCLC. Thus, targeting the MTA1-TJP1 axis may be a promising strategy for inhibiting NSCLC metastasis.

Supplementary material

Supplementary Fig. 1. (A) The level of MTA1 protein expression is the highest in H1299 cells and the lowest in H1734 cells. Representative images of Western Blot bands are shown. (B) Quantitative analysis of (A). Error bars represent *SD* from 3 repeats, *t*-test, $^{**}P < 0.01$. (C) MTA1 is knocked out by sgMTA1-#1 and sgMTA1-#2. Representative images of Western Blot bands are shown. (D) Quantitative analysis of (C). Error bars represent *SD* from 3 repeats, *t*-test, $^{**}P < 0.01$. (E) Successful construction of A549 cells with MTA1 overexpression. Representative images of Western Blot bands are shown. (F) Quantitative analysis of (E). Error bars represent *SD* from 3 repeats, *t*-test, $^{**}P < 0.01$. (G) Quantitative analysis of the level of MTA1 mRNA expression (data from 3 independent replicates, with 3 replicate wells), *t*-test, $^{**}P < 0.01$. (H) The level of TJP1 protein expression is the highest in H1734 cells and the lowest in H838 cells. Representative images of Western Blot bands are shown. (I) Quantitative analysis of (H). Error bars represent *SD* from 3 repeats, *t*-test, $^{**}P < 0.01$, $^{*}P < 0.05$.

(J) Western Blot confirms TJP1 knockdown in H1299 cells. Representative images of Western Blot bands are shown. (K) Quantitative analysis of (J). Error bars represent *SD* from 3 repeats, *t*-test, $^{**}P < 0.01$.

Declaration of Competing Interest

The authors declare that they have no competing interests.

CRediT authorship contribution statement

Wei Wang: Conceptualization, Formal analysis, Investigation, Methodology, Software, Writing – original draft, Writing – review & editing. **Mingsheng Ma:** Data curation, Investigation, Methodology, Writing – review & editing. **Li Li:** Conceptualization, Data curation, Formal analysis, Investigation, Methodology, Writing – original draft, Writing – review & editing, Funding acquisition. **Yunchao Huang:** Conceptualization, Formal analysis, Writing – review & editing. **Guangqiang Zhao:** Conceptualization, Formal analysis, Writing – review & editing. **Yongchun Zhou:** Conceptualization, Formal analysis, Writing – review & editing. **Yantao Yang:** Data curation, Investigation. **Yichen Yang:** Data curation, Investigation. **Biying Wang:** Data curation, Investigation. **Lianhua Ye:** Funding acquisition, Methodology, Resources, Supervision.

Acknowledgments

This research was supported by the following funds: Yunnan Fundamental Research Projects (No. 202101AY070001-159 and NO. 202201AY070001-135); National Natural Science Foundation of China (No. 81860325) and High-level health technical personnel of Yunnan Provincial Health Commission (No. L-2017006).

Supplementary materials

Supplementary material associated with this article can be found, in the online version, at doi:10.1016/j.tranon.2022.101500.

References

[1] H. Sung, J. Ferlay, R.L. Siegel, et al., Global cancer statistics 2020: GLOBOCAN estimates of incidence and mortality worldwide for 36 cancers in 185 countries, CA Cancer J. Clin. 71 (3) (2021) 209–249.
[2] H.W. Lv, W.Q. Xing, Y.F. Ba, H.M. Li, H.R. Wang, Y. Li, SMYD3 confers cisplatin chemoresistance of NSCLC cells in an ANKHD1-dependent manner, Transl. Oncol. 14 (2021), 101075, https://doi.org/10.1016/j.tranon.2021.101075.
[3] S.J. Wu, A. Arundhathi, H.C. Wang, C.Y. Chen, T.M. Cheng, S.F. Yuan, Y.M. Wang, Migration and invasion of NSCLC suppressed by the downregulation of Src/focal adhesion kinase using single, double and tetra domain anti- CEACAM6 antibodies, Transl. Oncol. 14 (2021), 101057, https://doi.org/10.1016/j.tranon.2021.101057.
[4] Y. Toh, S.D. Pencil, G.L. Nicolson, A novel candidate metastasis-associated gene, mta1, differentially expressed in highly metastatic mammary adenocarcinoma cell lines. cDNA cloning, expression, and protein analyses, J. Biol. Chem. 269 (1994) 22958–22963.
[5] R.A. Wang, MTA1–a stress response protein: a master regulator of gene expression and cancer cell behavior, Cancer Metastasis Rev. 33 (2014) 1001–1009, https://doi.org/10.1007/s10555-014-9525-1.
[6] N. Sen, B. Gui, R. Kumar, Role of MTA1 in cancer progression and metastasis, Cancer Metastasis Rev. 33 (2014) 879–889, https://doi.org/10.1007/s10555-014-9515-3.
[7] S. Deivendran, H. Marzook, T.R. Santhoshkumar, R. Kumar, M.R. Pillai, Metastasis-associated protein 1 is an upstream regulator of DNMT3a and stimulator of insulin-growth factor binding protein-3 in breast cancer, Sci. Rep. 7 (2017) 44225, https://doi.org/10.1038/srep44225.

[8] S. Salot, R. Gude, MTA1-mediated transcriptional repression of SMAD7 in breast cancer cell lines, Eur. J. Cancer 49 (2013) 492–499, https://doi.org/10.1016/j.ejca.2012.06.019.
[9] L. Deng, J. Tang, H. Yang, C. Cheng, S. Lu, R. Jiang, B. Sun, MTA1 modulated by miR-30e contributes to epithelial-to-mesenchymal transition in hepatocellular carcinoma through an ErbB2-dependent pathway, Oncogene 36 (2017) 3976–3985, https://doi.org/10.1038/onc.2016.491.
[10] M. Ishikawa, M. Osaki, M. Yamagishi, K. Onuma, H. Ito, F. Okada, H. Endo, Correlation of two distinct metastasis-associated proteins, MTA1 and S100A4, in angiogenesis for promoting tumor growth, Oncogene 38 (2019) 4715–4728, https://doi.org/10.1038/s41388-019-0748-z.
[11] W. Wang, Z. Hu, M. Ma, H. Yin, Y. Huang, G. Zhao, X. Cui, Q. Sun, Y. Yang, Y. Yang, et al., MTA1 expression can stratify the risk of patients with multifocal non-small cell lung cancers ≤3cm, Ther. Clin. Risk Manag. 17 (2021) 1295–1304, https://doi.org/10.2147/TCRM.S331317.
[12] S.D. Deodhar, K. James, T. Chiang, M. Edinger, B.P. Barna, Inhibition of lung metastases in mice bearing a malignant fibrosarcoma by treatment with liposomes containing human C-reactive protein, Cancer Res. 42 (1982) 5084–5088.
[13] M. Yan, L. Sun, J. Li, H. Yu, H. Lin, T. Yu, F. Zhao, M. Zhu, L. Liu, Q. Geng, et al., RNA-binding protein KHSRP promotes tumor growth and metastasis in non-small cell lung cancer, J. Exp. Clin. Cancer Res. 38 (2019) 478, https://doi.org/10.1186/s13046-019-1479-2.
[14] S.K. Shishodia, J. Shankar, Proteomic analysis revealed ROS-mediated growth inhibition of Aspergillus terreus by shikonin, J. Proteomics 224 (2020), 103849, https://doi.org/10.1016/j.jprot.2020.103849.
[15] L. González-Mariscal, A. Domínguez-Calderón, A. Raya-Sandino, J.M. Ortega-Olvera, O. Vargas-Sierra, G. Martínez-Revollar, Tight junctions and the regulation of gene expression, Semin. Cell Dev. Biol. 36 (2014) 213–223, https://doi.org/10.1016/j.semcdb.2014.08.009.
[16] O. Tornavaca, M. Chia, N. Dufton, L.O. Almagro, D.E. Conway, A.M. Randi, M. A. Schwartz, K. Matter, M.S. Balda, ZO-1 controls endothelial adherens junctions, cell-cell tension, angiogenesis, and barrier formation, J. Cell Biol. 208 (2015) 821–838, https://doi.org/10.1083/jcb.201404140.
[17] B. Manavathi, R. Kumar, Metastasis tumor antigens, an emerging family of multifaceted master coregulators, J. Biol. Chem. 282 (2007) 1529–1533, https://doi.org/10.1074/jbc.R600029200.
[18] R.R. Singh, R. Kumar, MTA family of transcriptional metaregulators in mammary gland morphogenesis and breast cancer, J. Mammary Gland Biol. Neoplasia 12 (2007) 115–125, https://doi.org/10.1007/s10911-007-9043-7.
[19] T. Zhan, N. Rindtorff, J. Betge, M.P. Ebert, M. Boutros, CRISPR/Cas9 for cancer research and therapy, Semin. Cancer Biol. 55 (2019) 106–119, https://doi.org/10.1016/j.semcancer.2018.04.001.
[20] S.B. Pakala, S.K. Rayala, R.A. Wang, K. Ohshiro, P. Mudvari, S.D. Reddy, Y. Zheng, R. Pires, S. Casimiro, M.R. Pillai, et al., MTA1 promotes STAT3 transcription and pulmonary metastasis in breast cancer, Cancer Res. 73 (2013) 3761–3770, https://doi.org/10.1158/0008-5472.CAN-12-3998.
[21] Y. Zhang, H.H. Ng, H. Erdjument-Bromage, P. Tempst, A. Bird, D. Reinberg, Analysis of the NuRD subunits reveals a histone deacetylase core complex and a connection with DNA methylation, Genes Dev. 13 (1999) 1924–1935, https://doi.org/10.1101/gad.13.15.1924.
[22] S. Balasenthil, A.E. Gururaj, A.H. Talukder, R. Bagheri-Yarmand, T. Arrington, B. J. Haas, J.C. Braisted, I. Kim, N.H. Lee, R. Kumar, Identification of Pax5 as a target of MTA1 in B-cell lymphomas, Cancer Res. 67 (2007) 7132–7138, https://doi.org/10.1158/0008-5472.CAN-07-0750.
[23] A.E. Gururaj, R.R. Singh, S.K. Rayala, C. Holm, P. den Hollander, H. Zhang, S. Balasenthil, A.H. Talukder, G. Landberg, R. Kumar, MTA1, a transcriptional activator of breast cancer amplified sequence 3, Proc. Natl. Acad. Sci. U. S. A. 103 (2006) 6670–6675, https://doi.org/10.1073/pnas.0601989103.
[24] S.B. Pakala, S. Reddy, T.M. Bui-Nguyen, S.S. Rangparia, A. Bommana, R. Kumar, MTA1 coregulator regulates LPS response via MyD88-dependent signaling, J. Biol. Chem. 285 (2010) 32787–32792, https://doi.org/10.1074/jbc.M110.151340.
[25] Y. Toh, S. Kuninaka, K. Endo, T. Oshiro, Y. Ikeda, H. Nakashima, H. Baba, S. Kohnoe, T. Okamura, G.L. Nicolson, et al., Molecular analysis of a candidate metastasis-associated gene, MTA1: possible interaction with histone deacetylase 1, J. Exp. Clin. Cancer Res. 19 (2000) 105–111.
[26] A. Simpson, J. Uitto, U. Rodeck, M.G. Mahoney, Differential expression and subcellular distribution of the mouse metastasis-associated proteins Mta1 and Mta3, Gene 273 (2001) 29–39, https://doi.org/10.1016/s0378-1119(01)00563-7.
[27] J. Liu, D. Xu, H. Wang, Y. Zhang, Y. Chang, J. Zhang, J. Wang, C. Li, H. Liu, M. Zhao, et al., The subcellular distribution and function of MTA1 in cancer differentiation, Oncotarget 5 (2014) 5153–5164, https://doi.org/10.18632/oncotarget.2095.
[28] E.A. Runkle, D. Mu, Tight junction proteins: from barrier to tumorigenesis, Cancer Lett. 337 (2013) 41–48, https://doi.org/10.1016/j.canlet.2013.05.038.
[29] Y.E. Kim, M. Won, S.G. Lee, C. Park, C.H. Song, K.K. Kim, RBM47-regulated alternative splicing of TJP1 promotes actin stress fiber assembly during epithelial-to-mesenchymal transition, Oncogene 38 (2019) 6521–6536, https://doi.org/10.1038/s41388-019-0892-5.
[30] L. Kondratyeva, I. Chernov, E. Kopantzev, D. Didych, A. Kuzmich, I. Alekseenko, S. Kostrov, E. Sverdlov, Pancreatic lineage specifier PDX1 increases adhesion and decreases motility of cancer cells, Cancers 13 (2021), https://doi.org/10.3390/cancers13174390 (Basel).
[31] V. Gkretsi, T. Stylianopoulos, Cell adhesion and matrix stiffness: coordinating cancer cell invasion and metastasis, Front. Oncol. 8 (2018) 145, https://doi.org/10.3389/fonc.2018.00145.